Electronic Supplementary Material (ESI) for Nanoscale.

SUPPLEMENTARY MATERIAL

A Family of Superconducting Boron Crystals Made of Stacked Bilayer Borophenes

Yuewen Mu[†]*, Bao-Tian Wang[‡], Si-Dian Li*[,†] and Feng Ding*[,¶]

[†]*Key Laboratory of Materials for Energy Conversion and Storage of Shanxi Province, Institute of Molecular Science, Shanxi University, Taiyuan, 030006, China*

[‡]*Spallation Neutron Source Science Center, Institute of High Energy Physics, Chinese Academy of Sciences (CAS), Dongguan, Guangdong 523803, China*

[¶]*Centre for Multidimensional Carbon Materials, Institute for Basic Science, Ulsan, South Korea*

E-mail: ywu@sxu.du.cn; *lisidian@sxu.edu.cn*; *f.ding@unist.ac.kr*

Table S1: The k-meshes and q-meshes for phonon (PH) and electron-phonon coupling (EPC) calculations, and calculated EPC constants λ, logarithmic average of frequency ω_{log}, superconducting critical temperature T_c. The effective screened Coulomb repulsion constant (μ^*) and Methfessel-Paxton smearing width for sum over q in T_c calculations are 0.1 and 0.2 meV, respectively.

Allotrope	k-mesh for EPC	k-mesh for PH	q-mesh	λ	ω_{log} (K)	T_c (K)
$\delta_{6\text{-}B_6}$	36×36×24	18×18×12	6×6×4	0.516	727.375	9.977
$\delta_{6\text{-}B_6}$	48×48×32	24×24×16	6×6×4	0.539	705.359	11.339
$\delta_{6\text{-}B_6}$	60×60×40	30×30×20	6×6×4	0.539	706.705	11.394
$\delta_{6\text{-}\mathbf{B_6}}$	**32×32×24**	**16×16×12**	**8×8×6**	**0.523**	**702.332**	**10.146**
$\beta_{12\text{-}B_5}$	48×48×24	24×24×12	8×8×4	0.534	615.680	9.585
$\beta_{12\text{-}B_5}$	64×64×32	32×32×16	8×8×4	0.534	616.655	9.632
$\beta_{12\text{-}\mathbf{B_5}}$	40×40×24	20×20×12	10×10×6	0.522	642.822	**9.226**
$\beta_{12\text{-}\mathbf{B_5}}$	**56×56×32**	**28×28×16**	**14×14×8**	**0.532**	**608.963**	**9.360**
$\beta_{12\text{-}\mathbf{B_5}}$ **(100 GPa)**	40×40×24	20×20×12	10×10×6	0.574	653.129	**13.031**
$\delta_{3\text{-}B_4}$	32×32×24	16×16×12	8×8×6	0.453	664.982	5.313
$\delta_{3\text{-}B_4}$	48×48×36	24×24×18	8×8×6	0.455	674.009	5.488
$\delta_{3\text{-}\mathbf{B_4}}$	**40×40×32**	**20×20×16**	**10×10×8**	**0.460**	**660.871**	**5.647**

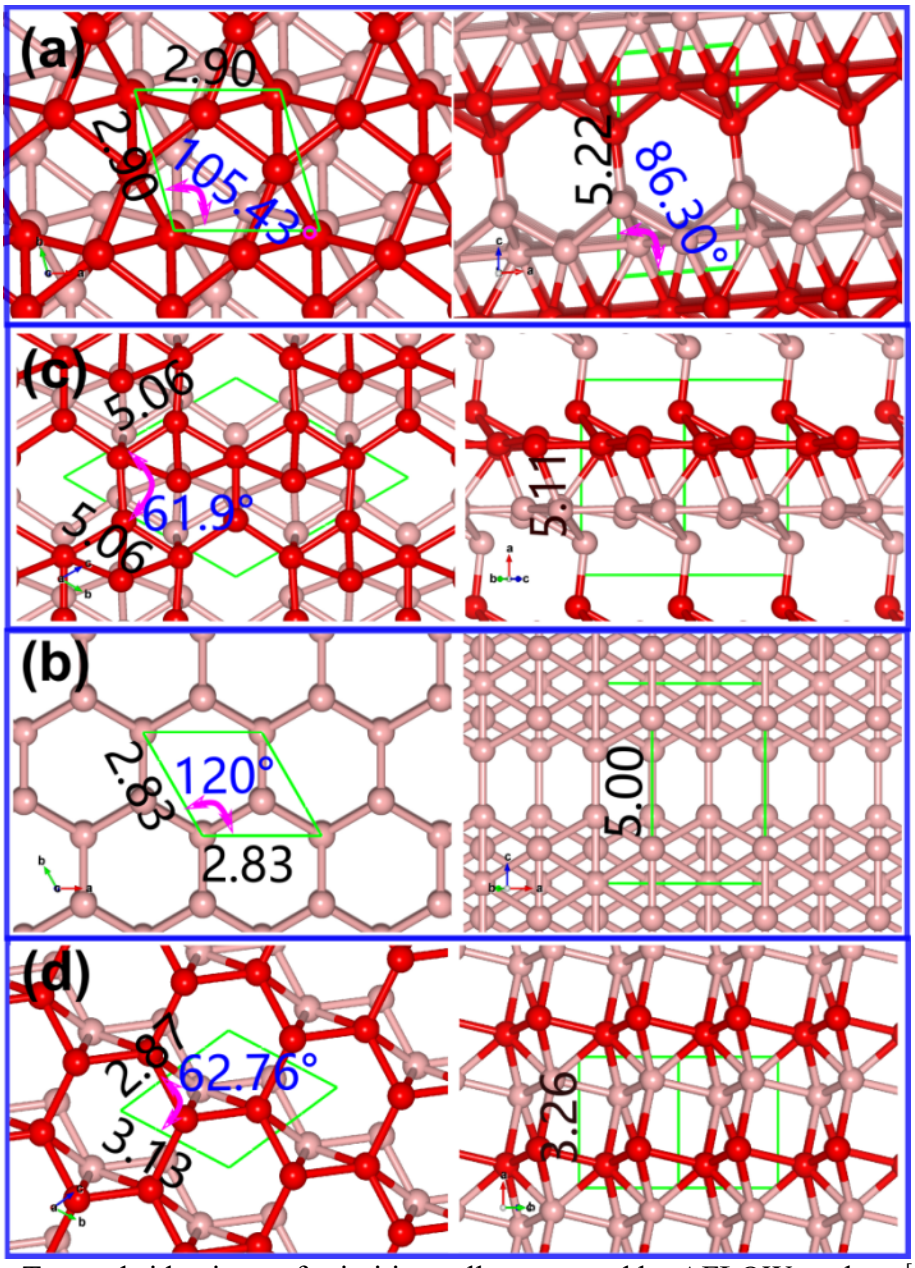

Figure S1. Top and side views of primitive cells converted by AFLOW package[1] for proposed allotropes (a) $^{\delta_6}$-B_6, (b) $^{\alpha}$-B_{16}, (c) $^{\beta_{12}}$-B_5 and (d) $^{\delta_3}$-B_4.

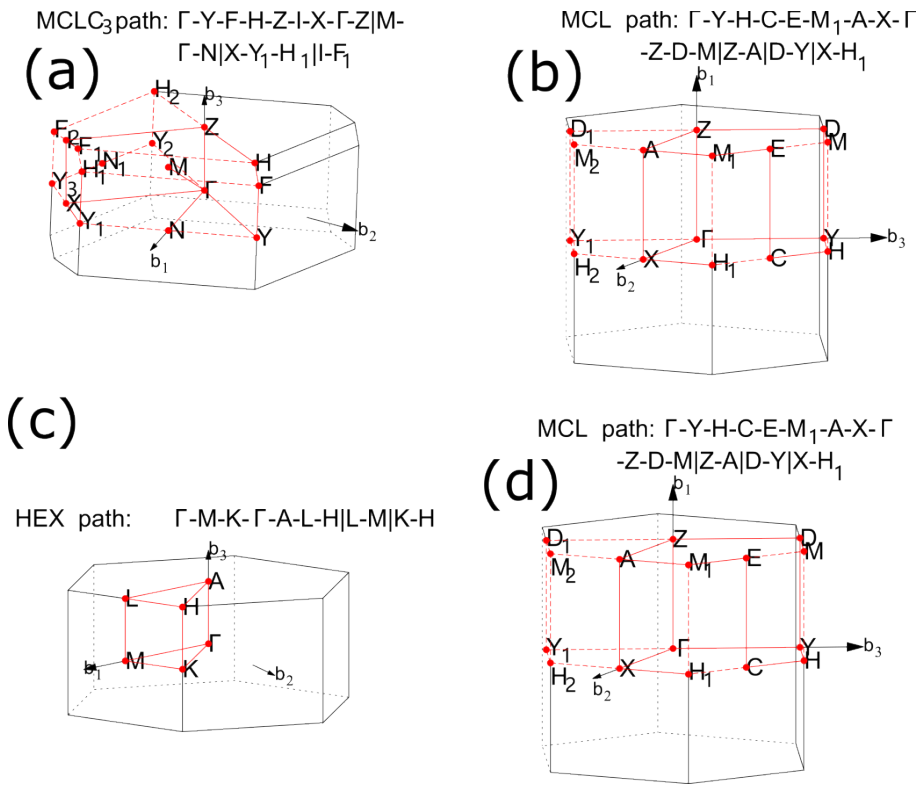

Figure S2. First Brillouin zones for (a) δ_6-B_6, (b) α-B_{16}, (c) β_{12}-B_5 and (d) δ_3-B_4 allotropes generated by AFLOW package[1].

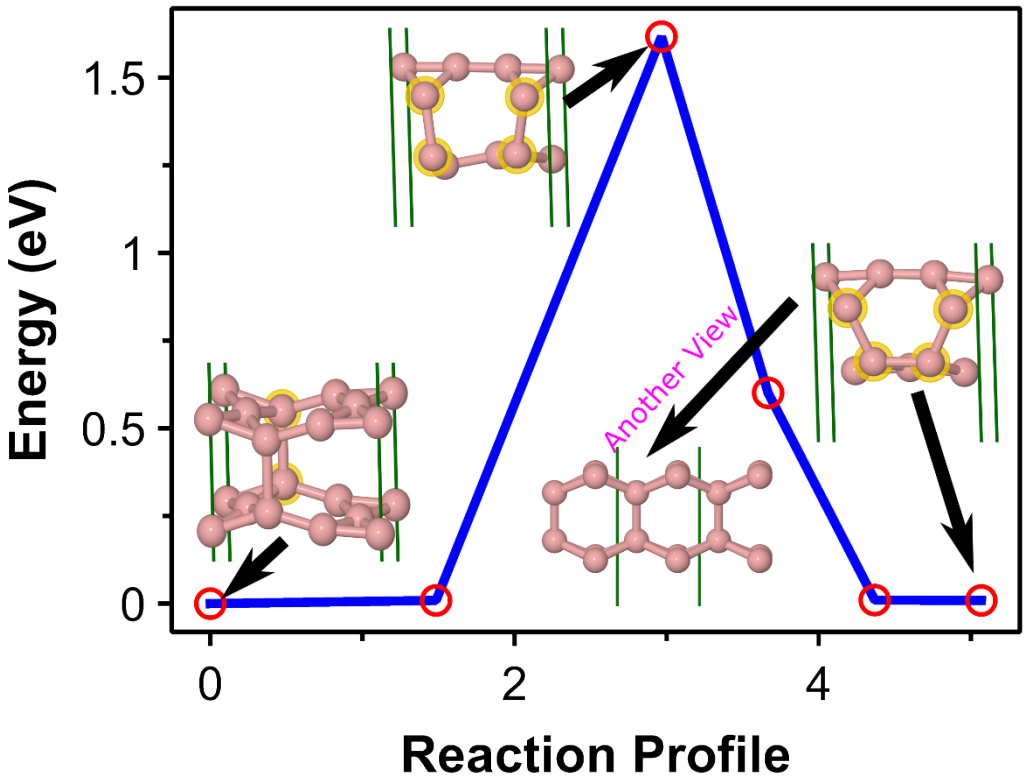

Figure S3. Phase transition from the free-standing bilayer β_{12} borophene to the β_{12}-B_5 bilayer unit. Key connections are marked in halos to illustrate transition details.

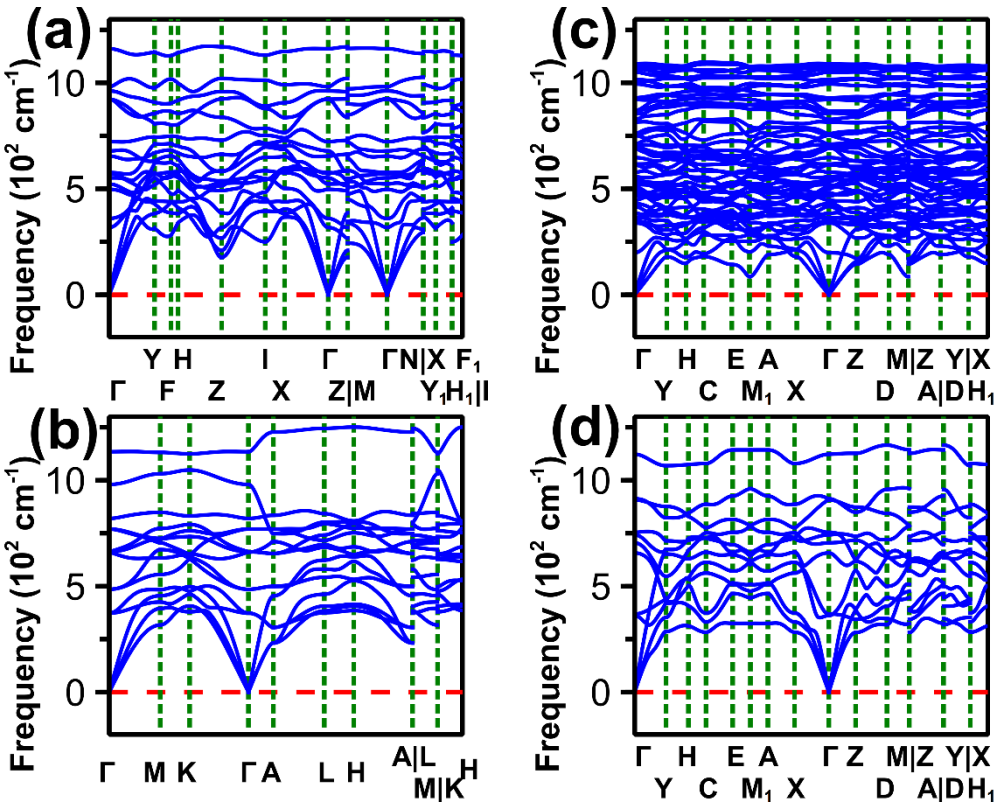

Figure S4. Phonon spectra of (a) $^{\delta_6}$-B_6, (b) $^{\alpha}$-B_{16}, (c) $^{\beta_{12}}$-B_5 and (d) $^{\delta_3}$-B_4 allotropes by Phonopy program with $3 \times 3 \times 3$ supercells.

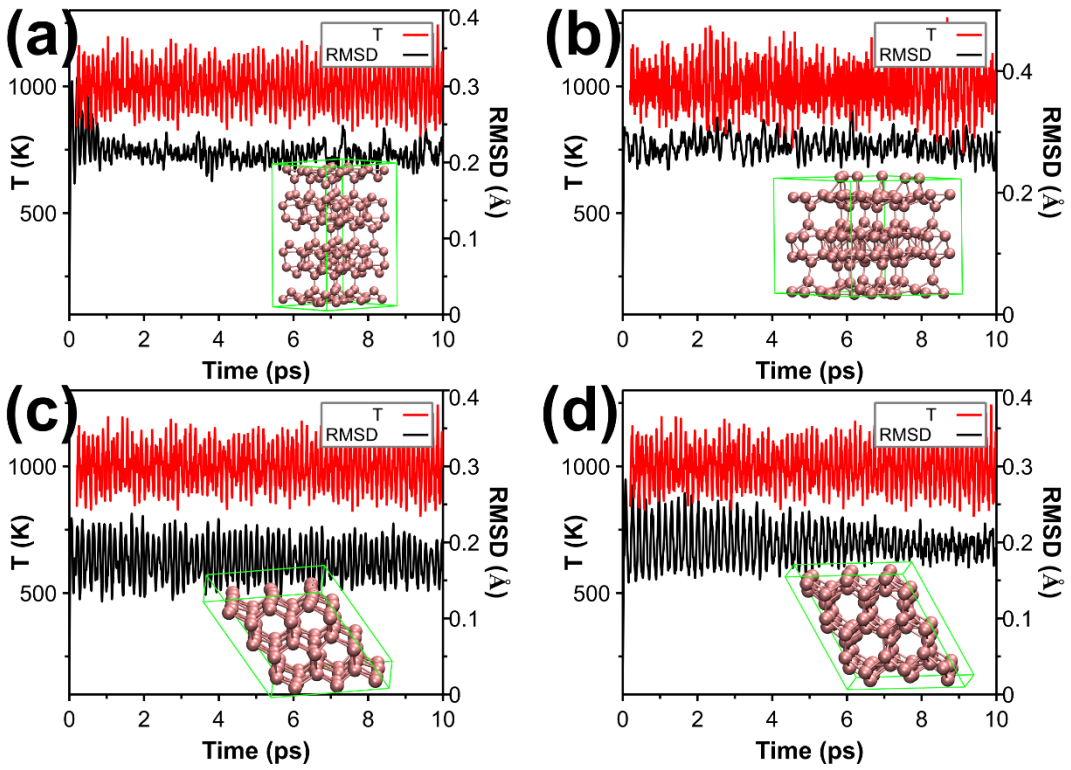

Figure S5. The evolution of the temperatures and root mean square deviations (RMSD) in the BOMD simulations at 1000 K (10 ps) for proposed allotropes (a) $^{\delta_6}$-B_6, (b) $^{\alpha}$-B_{16}, (c) $^{\beta_{12}}$-B_5 and (d) $^{\delta_3}$-B_4. The RMSD is calculated using VMD package[2]. The snapshots for their last frames are shown as insets.

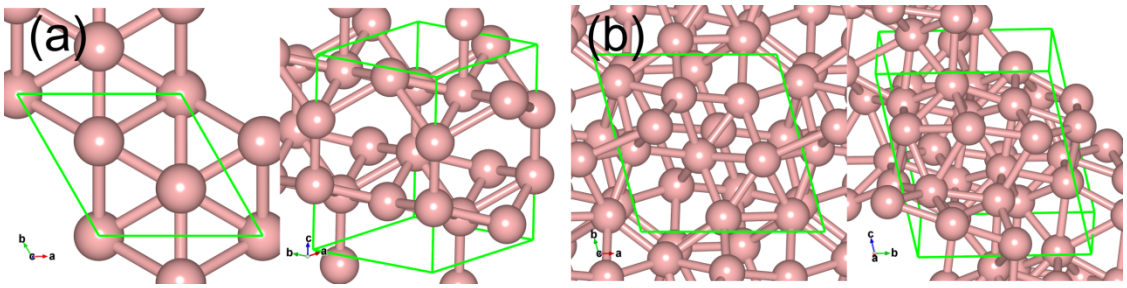

Figure S6. Top and side views of high-pressure phases of (a) $^{\delta_6}$-B_6 and (b) $^{\alpha}$-B_{16} at 200 GPa.

Table S2: Main elastic constants (GPa), Voigt-Reuss-Hill (VRH) average[3] bulk modulus B (Gpa), shear modulus G (GPa), Young's Modulus Y (GPa), Poisson's ratio ν, Pugh's modulus ratio $\kappa = G/B$[4] and mechanical stabilities for proposed allotropes, α-Ga, α-rh and γ-B_{28} phases. The formulas to calculate bulk modulus, shear modulus, Young's Modulus and Poisson's ratio within the Voigt and Reuss bounds for the allotropes are from Ref. 5 and Ref. 6. The mechanical stability criteria to be satisfied for the allotropes come from Ref. 5 and Ref. 7.

Allotrope	δ_{6}-B_6	α-B_{16}	β_{12}-B_5	δ_{3}-B_4	α-Ga	α-rh	γ-B_{28}
C_{11}	442.23	464.13	439.95	606.30	644.66	594.35	615.06
C_{12}	171.68	199.01	159.12	86.09	89.46	71.46	85.67
C_{13}	84.81	-6.22	37.57	142.83	114.22	51.36	41.10
C_{22}	466.19	451.83	439.95	503.30	770.24	485.05	548.93
C_{23}	80.74	56.91	37.57	163.90	-2.72	94.63	86.89
C_{33}	599.24	428.34	877.53	500.51	690.36	512.69	462.17
C_{44}	179.01	99.52	204.49	137.99	265.40	170.69	245.73
C_{55}	157.02	88.02	204.49	213.57	375.27	214.61	226.56
C_{66}	276.85	172.95	140.42	231.93	262.15	224.78	256.06
B	239.15	198.51	242.29	255.49	279.04	226.97	226.40
G	188.67	126.07	198.78	180.60	303.19	205.15	238.65
Y	448.15	312.14	468.28	438.48	667.73	472.96	529.79
ν	0.19	0.24	0.18	0.21	0.10	0.15	0.11
κ	1.27	1.57	1.22	1.41	0.92	1.11	0.95
Mechanical Stability	Stable	Stable	Stable	Stable	Stable	Stable	Stable

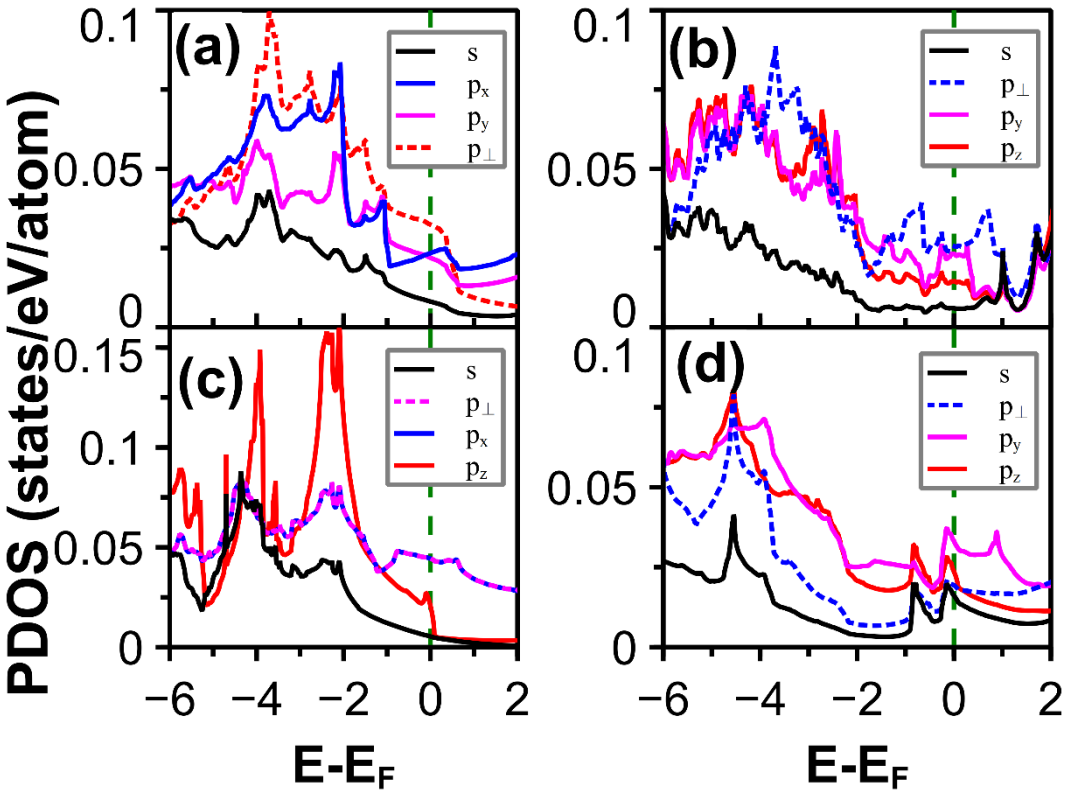

Figure S7. Projected density of states (PDOS) for proposed allotropes (a) $^{\delta_6}$-B$_6$, (b) $^{\alpha}$-B$_{16}$, (c) $^{\beta_{12}}$-B$_5$ and (d) $^{\delta_3}$-B$_4$ at PBE level. $^{p_\perp}$ stands for p states basically perpendicular to the basal plane of precursor borophenes.

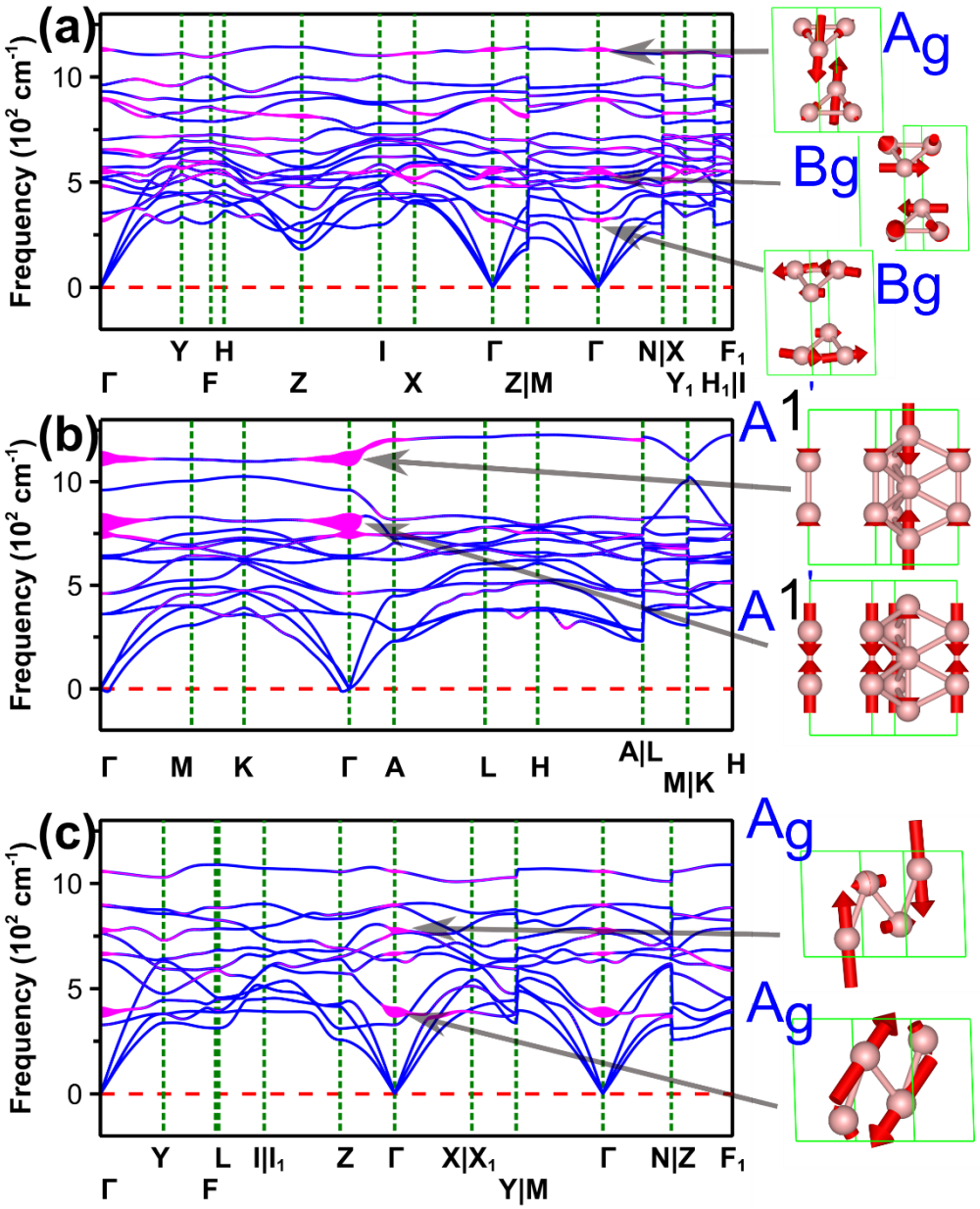

Figure S8. Phonon spectrum and electron−phonon coupling for proposed allotropes (a) $^{\delta_6}$-B$_6$, (b) $^{\beta_{12}}$-B$_5$ and (c) $^{\delta_3}$-B$_4$. The size of the magenta circles is proportional to the magnitude of electron−phonon couplings $\lambda_{q\nu}$. The modes with large couplings at Γ and their symmetries are also given. The lattice of $^{\delta_3}$-B$_4$ is a little distorted after reoptimization by Quantum ESPRESSO, so its high-symmetry K points are a little different from those used in VASP calculations, though their space group are the same.

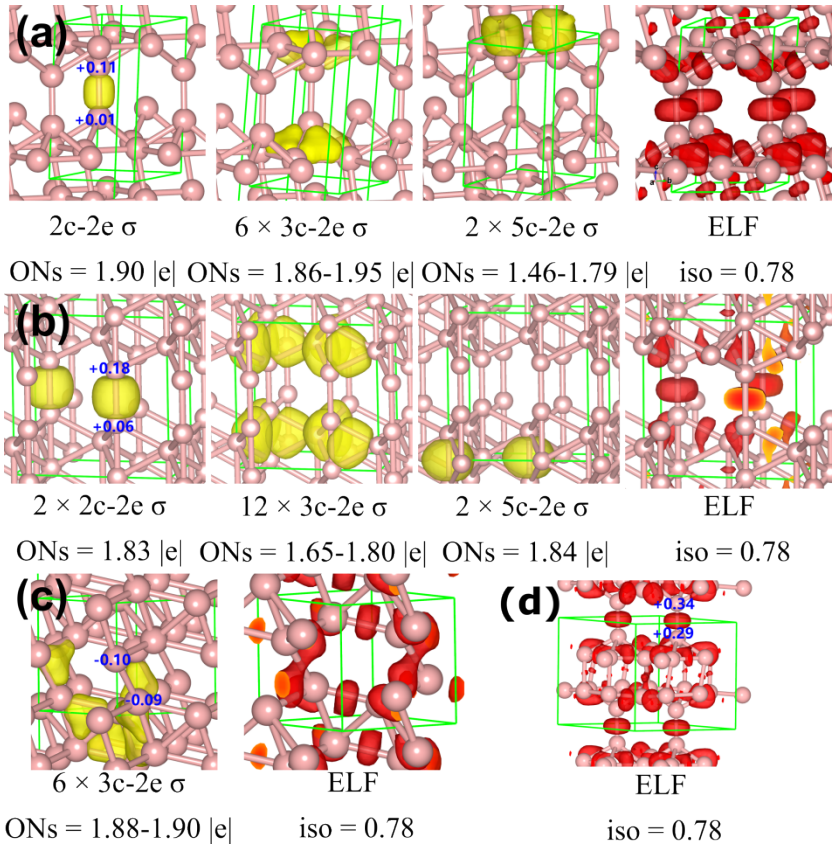

Figure S9. Solid state adaptive natural density partitioning (SSAdNDP) and electron localization function (ELF) plot for (a) $^{\delta}$$_{6}$-B$_{6}$, (b) $^{\beta}$$_{12}$-B$_{5}$, (c) $^{\delta}$$_{3}$-B$_{4}$ and (d) $^{\alpha}$-B$_{16}$ (without SSAdNDP). It should be pointed out that the primitive $^{\beta}$$_{12}$-B$_{5}$ with odd electrons (15 *e*) are converted to an orthogonal cell with even electrons (30 *e*) for bonding analysis. Due to incomplete occupation, 16 multi-center bonds with high occupied numbers (ONs) are proposed for $^{\beta}$$_{12}$-B$_{5}$ allotrope, which is strongly supported by the ELF plot. The Bader charges for some atoms are labeled in blue.

Reference

[1] Curtarolo, S.; Setyawan, W.; Hart, G. L. W.; Jahnatek, M.; Chepulskii, R. V.; Taylor, R. H.; Wang, S.; Xue, J.; Yang, K.; Levy, O.; Mehl, M. J.; Stokes, H. T.; Demchenko, D. O.; Morgan, D. AFLOW: An Automatic Framework for High-Throughput Materials Discovery. *Comp. Mater. Sci.* **2012**, *58*, 218–226.

[2] Humphrey, W.; Dalke, A.; Schulten, K. VMD: Visual Molecular Dynamics. *J. Mol. Graph.* **1996**, *14*, 33–38.

[3] Hill, R. The Elastic Behaviour of a Crystalline Aggregate. *Proc. Phys. Soc. A* **1952**, *65*, 349–354.

[4] Pugh, S. F. Xcii. Relations Between the Elastic Moduli and the Plastic Properties of Polycrystalline Pure Metals. *Philos. Mag.* **1954**, *45*, 823–843.

[5] Wu, Z.; Zhao, E.; Xiang, H.; Hao, X.; Liu, X.; Meng, J. Crystal Structures and Elastic Properties of Superhard IrN_2 and IrN_3 from First Principles. *Phys. Rev. B* **2007**, *76*, 054115.

[6] Watt, J. P.; Peselnick, L. Clarification of the Hashin-Shtrikman Bounds on the Effective Elastic Moduli of Polycrystals with Hexagonal, Trigonal, and Tetragonal Symmetries. *J. Appl. Phys.* **1980**, *51*, 1525–1531.

[7] Mouhat, F.; Coudert, F.-X. Necessary and Sufficient Elastic Stability Conditions in Various Crystal Systems. *Phys. Rev. B* **2014**, *90*, 224104.